Hook3 interacts with PCM1 to regulate pericentriolar material assembly and the timing of neurogenesis

Xuecai Ge[1,2,3], **Christopher L. Frank**[1,2], **Froylan Calderon de Anda**[1,2], and **Li-Huei Tsai**[1,2,4,#]

[1]Picower Institute for Learning and Memory, Department of Brain and Cognitive Sciences, Massachusetts Institute of Technology, 77 Massachusetts Avenue, Building 46, Room 4235A, Cambridge, MA 02139, USA

[2]Howard Hughes Medical Institute, 77 Massachusetts Avenue, Building 46, Room 4235A, Cambridge, MA 02139, USA

[3]Program in Neuroscience, Harvard Medical School, Boston, MA 02115, USA

[4]The Stanley Center for Psychiatric Research, Broad Institute of Harvard and Massachussetts Institute of Technology, Cambridge, MA 02139, USA

SUMMARY

Centrosome functions are important in multiple brain developmental processes. Proper functioning of the centrosome relies on assembly of protein components into the pericentriolar material. This dynamic assembly is mediated by the trafficking of pericentriolar satellites, which are comprised of centrosomal proteins. Here we demonstrate that trafficking of pericentriolar satellites requires the interaction between Hook3 and Pericentriolar Material 1 (PCM1). Hook3, previously shown to link the centrosome and the nucleus in *C. elegans*, is recruited to pericentriolar satellites through interaction with PCM1, a protein associated with schizophrenia. Disruption of the Hook3-PCM1 interaction *in vivo* impairs interkinetic nuclear migration, a featured behavior of embryonic neural progenitors. This in turn leads to overproduction of neurons and premature depletion of the neural progenitor pool in the developing neocortex. These results underscore the importance of centrosomal assembly in neurogenesis, and provide potential insights into the etiology of brain developmental diseases related to the centrosome dysfunction.

INTRODUCTION

Centrosome functions are important for multiple processes during embryonic brain development, including neuronal migration, neural polarity establishment, and neurogenesis (Badano et al., 2005; Higginbotham and Gleeson, 2007). Therefore, understanding the formation and function of the centrosome in embryonic brains will provide helpful insights into the regulation of these brain developmental processes. Electron microscopy studies revealed that the centrosome consists of a pair of centrioles and the pericentriolar material. The latter is a meshwork of various proteins intertlaced into a well-organized matrix (Bettencourt-Dias and Glover, 2007; Doxsey, 2001b). Most centrosomal functions are thought to be carried

out in the pericentriolar material, including microtubule nucleation, microtubule anchorage, and mitotic spindle organization (Luders and Stearns, 2007; Rieder et al., 2001). The pericentriolar material is structurally very dynamic. Individual constituent proteins, such as centrin, pericentrin and ninein, undergo vigorous exchange between the centrosome-bound pool and a larger cytoplasmic pool (Doxsey, 2001a; Young et al., 2000). Consistent with this observation, many pericentriolar material components are not confined to centrioles, but are distributed in the cytoplasm and the nucleus (Baron et al., 1994; Paoletti et al., 1996). Furthermore, Fluorescence Recovery After Photobleaching (FRAP) experiments revealed rapid turnover of multiple centrosomal proteins (Khodjakov and Rieder, 1999; Valente et al., 2006). Maintenance of the structural dynamics depends on pericentriolar satellites, non-membranous granules with a diameter of 70-100nm, where were first observed as electron-dense vesicles by electron microscopy (Berns et al., 1977). Pericentriolar satellites shuttle between the centrosome and the cytoplasm, and may mediate the transport of proteins destined for the pericentriolar material (Kubo et al., 1999; Zimmerman and Doxsey, 2000).

The first identified molecular component of pericentriolar satellites was Pericentriolar Material 1 (PCM1) (Balczon et al., 1994; Baron and Salisbury, 1988). PCM1 serves as a scaffold protein and recruits various centrosomal proteins to pericentriolar satellites (Hames et al., 2005), which are then linked to dynein motors via the Bardet–Biedl syndrome 4 protein (Kim et al., 2004). Dynein motor complexes then transport pericentriolar satellites along microtubules towards the centrosome (Kubo et al., 1999). Compromising PCM1 function impairs the proper functioning of pericentriolar satellites, resulting in a reduction of protein integration into the centrosome (Dammermann and Merdes, 2002). Recently, PCM1 was discovered to be highly associated with schizophrenia in human genetic studies (Datta et al., 2008; Gurling et al., 2006; Kamiya et al., 2008). Furthermore, it interacts with and functions at the centrosome in cooperation with DISC1, another risk gene of schizophrenia (Kamiya et al., 2008). Although accumulating data suggest that brain developmental disorders, in particular, defects in cortical neural progenitor proliferation, contribute to the onset of this psychiatric disorder (Mao et al., 2009; Ross et al., 2006), whether PCM1 is involved in embryonic brain development is largely unknown.

In the developing neocortex, neural progenitor cells (radial glia and neuroepithelial cells) proliferate to establish a pool from which all neurons are generated. These neural progenitors reside in the ventricular zone (VZ), a pseudostratified columnar epithelium that lines the lateral ventricle. The neural progenitor pool replenishes itself during development, and this self-replenishment must be balanced with neurogenesis in order to ensure that a precise number of neurons are generated. Disrupting this balance results in severe neurological and neuropsychiatric disorders, ranging from microcephaly to bipolar disorder and schizophrenia (Badano et al., 2005; Mao et al., 2009). Interestingly, nuclei of neural progenitors oscillate within the VZ in correlation with cell cycle progression in a process termed interkinetic nuclear migration (INM) (Sauer, 1935). During INM, neural progenitors undergo mitosis along the ventricular surface. After mitosis, nuclei ascend to the basal end of the VZ, where cells duplicate their DNA during S phase. Subsequently, nuclei descend towards the apical side of the VZ and cells undergo mitosis (Sauer, 1935). INM has been suggested to regulate the balance between neurogenesis and maintenance of the neural progenitor pool by controlling the exposure of progenitor cells to neurogenic versus proliferative signals (Del Bene et al., 2008; Murciano et al., 2002). INM is regulated by microtubules, actin, and microtubule-associated proteins (Messier and Auclair, 1974; Tsai et al., 2005; Webster and Langman, 1978), and the centrosomal proteins Cep120 and TACC regulate INM by controlling the length of microtubules that attach to the centrosome (Xie et al., 2007). This underscores an essential function of the centrosome in the regulation of neural progenitor proliferation.

In embryonic neural progenitors, the centrosome resides at the ventricular surface when the nucleus undergoes ascending and descending movements during INM. PCM1-containing pericentriolar satellites are found at the apical surface of various epithelial cells, including neuroepithelia in the developing neocortex (Cohen et al., 1988; Kubo et al., 1999). However, it remains unknown whether PCM1-mediated centrosomal assembly is involved in cortical neurogenesis. Here, we demonstrate that pericentriolar satellite-mediated protein trafficking is essential for maintenance of proper centrosome function in neural progenitors. We found that trafficking of pericentriolar satellites relies on the interaction between PCM1 and Hook3. Hook3 is the mammalian homolog of *C. elegans* ZYG-12 that links the centrosome and the nucleus (Malone et al., 2003). In mammals, Hook3 is recruited to pericentriolar satellites through an interaction with PCM1.

Disrupting this interaction impairs trafficking of pericentriolar satellites and subsequently reduces protein assembly at the centrosome. This in turn compromises centrosome functions, including its ability to organize the microtubule cytoskeleton. Finally, silencing Hook3 or PCM1, or blocking the Hook3-PCM1 interaction *in vivo*, impairs INM, resulting in an over-production of neurons at the expense of neural progenitor pool. Our findings have broad implications in the understanding of centrosomal protein assembly during embryonic neurogenesis. Furthermore, it provides potential insight into the development of centrosome-related neural developmental disorders.

RESULTS

Mouse Hook3 localizes to the centrosomal periphery

To evaluate centrosomal function during cortical development, we initiated our studies with Hook3, which has been reported to associate with the centrosome in *C. elegans*. Consistent with a role in neurogenesis, Hook3 is expressed in the developing mouse neocortex concurrent with neurogenesis (E11-E18, Figure 1A). Immunostaining of E14 cortical slices showed that Hook3 expression was relatively high in the VZ, where it overlapped with the neural progenitor marker nestin (Figure 1B). In particular, Hook3 fluorescence highlighted the apical edge of the VZ, where centrosomes of neural progenitors reside. Upon closer examination of the VZ apical surface, we found that Hook3 fluorescence covered the centrosome *per se* and was also distributed to the centrosome periphery (Figure 1C, D, *en face* view). To further elucidate the subcellular localization of Hook3, we examined Hook3 localization in a neuroblastoma cell line (N2A). Hook3 fluorescence appeared as small granules concentrated at the centrosome, but was also distributed throughout the cytoplasm (Figure 1E). This subcellular localization was also observed in primary cultured neural progenitors (Figure S1A). The nature of these granular structures will be addressed later.

Hook3 regulates embryonic neurogenesis by controlling INM

To study the function of Hook3, we developed two RNAi constructs, Hook3RNAi-1 and -2, to silence Hook3 expression. Both constructs efficiently knocked down endogenous Hook3 in N2A cells (Figure 2A, B) and in the mouse cerebral cortex (Figure 2C). We then introduced Hook3 RNAi into E11.5 mouse embryonic brains together with Venus (a variant of EYFP) by in utero electroporation, a technique that allows analysis of acute effects of silencing genes of interest, and examined the brains at E14.5.

As Hook3 is highly expressed in neural progenitors, we first examined the division of progenitors cells in the VZ by staining with phospho-histone H3 (PH3) antibody (Figure 2D). While most cells divide on the ventricular surface in control brain sections (Figure 2D, arrows), a significantly higher percentage of cells divide away from the ventricular surface after Hook3 knockdown (Figure 2D, E, arrowheads). We define apical division as mitoses that occur within

20μm of the ventricular surface (Miyama et al., 2001). Ectopic mitoses were rescued by co-electroporation with RNAi-resistant full-length Hook3 (Figure 2D). The observed ectopic mitoses suggest that INM is uncoupled from cell cycle progression, as reported by previous studies (Tsai et al., 2005; Xie et al., 2007).

We next sought to identify the responsible factor that elicited the uncoupling. We first examined cell cycle progression by FACS analysis, but did not find any abnormalities (Figure S2). Another possibility is that the phenotype is caused by an impairment in INM. To address this possibility, we first examined the morphology of transfected nuclei. As Sauer noticed in his original study, nuclei assume an elongated morphology along the apical-basal axis during INM. When INM halts or is impaired, nuclei exhibit rounded shapes (Chenn and McConnell, 1995; Sauer, 1935). To evaluate this, we measured the length and width of nuclei of transfected cells, and found that the length to width ratio was significantly smaller after Hook3 knockdown, suggesting that nuclei assume a less elongated morphology. This phenotype was rescued by RNAi-resistant Hook3 (Figure 2F, G). These results indicate that INM might be impaired after Hook3 knockdown.

To directly evaluate Hook3 function in INM, we performed time-lapse imaging on acute cortical slices two days after in utero electroporation (Figure 2I). In the VZ, newborn neurons migrate upward (away from the ventricular surface), with their cell bodies amidst cell bodies of neural progenitors undergoing INM. Therefore, we focused on the descending movement (toward the ventricular surface) of transfected cells in order to exclude migrating neuron from our analysis. During the 8 hour imaging period, most cell bodies of control cells traversed long distances (Figure 2H,J; movie S1), and some cells divided at the ventricular surface (Figure 2H, arrow). In contrast, cell bodies of most Hook3 RNAi transfected cells oscillated at their original positions (Figure 2H,J; movie S2) and divided away from the ventricular surface (Figure 2H, arrowhead). The reduced nuclear motility of Hook3 knockdown cells was restored by co-expressing RNAi-resistant Hook3 (Figure 2H,J; movie S3). Taken together, we conclude that Hook3 knockdown impairs INM.

Hook3 is necessary for maintenance of the neural progenitor pool

We next examined effects of Hook3 RNAi-mediated INM disruption on neurogenesis. At E14, neural progenitors predominantly undergo N-P divisions, in which one daughter cell differentiates into a neuron and the other remains a neural progenitor. In this way, neurons are continuously generated while the neural progenitor pool is maintained. To evaluate cell fate after ectopic divisions, we performed the cell cycle exit assay. Embryos were electroporated at E11.5, pulse-labeled with BrdU at E13.5, and analyzed at E14.5 by immunostaining for BrdU and Ki67 (labels cells in late G1, S, G2 and M-phase). We found that cells expressing Hook3 RNAi exhibited a significantly higher cell-cycle exit index compared to control cells (Figure 3A, B). In addition, transfected cells in Hook3 knockdown sections showed a significantly lower BrdU labeling index, which suggests a diminished size of the neural progenitor pool (Figure 3C).

In line with the increased cell cycle exit, neurogenesis significantly increased after Hook3 knockdown. This is first evidenced by the higher percentage of cells migrating to the CP/IZ, and lower percentage remaining in the VZ/SVZ (Figure 3D, E). Second, immunostaining of brain sections with neuron-specific markers Tuj1 and NeuN revealed that neurogenesis increased after Hook3 knockdown (Figure 3D, F; Figure S3D). Taken together, these data suggest that as a result of Hook3 knockdown-mediated INM disruption, cells differentiate into neurons after ectopic cell division, leading to premature depletion of the neural progenitor pool and overproduction of neurons.

Hook3 interacts with PCM1, a component of pericentriolar satellites

To elucidate the molecular mechanism by which Hook3 is involved in INM, we performed a yeast-two-hybrid screen for Hook3 interacting proteins. One potentially interesting interactor was PCM1 (Figure 4A), given that its subcellular localization resembles that of Hook3 in previous studies (Balczon et al., 1994; Baron and Salisbury, 1988; Kubo and Tsukita, 2003). Co-immunoprecipitation from E14 mouse brain lysates confirmed the interaction between PCM1 and Hook3 *in vivo* (Figure 4B). We then examined the subcellular localization of both proteins by over-expressing EGFP-Hook3 in N2A cells and staining with PCM1 antibody (Figure 4C,D). As previously reported (Kubo et al., 1999; Kubo and Tsukita, 2003), PCM1 immunofluorescence appears as granules concentrated at the centrosome, with a small proportion scattered in the cytoplasm. These granules overlapped with EGFP-Hook3, particularly in the vicinity of the centrosome (Figure 4D). Furthermore, we confirmed the colocalization of the two proteins by immuno-staining using Biotin-conjugated Hook3 antibody, followed by PCM1 staining (Figure S1C-C'). In the developing cortex, PCM1 immunofluorescence concentrates at the ventricular surface, where it overlaps with and surrounds the centrosome (Figure 4E-F). These results suggest that PCM1 might be a component of the molecular machinery containing Hook3 that regulates neurogenesis.

As PCM1 is a component of pericentriolar satellites (Baron and Salisbury, 1988), its co-localization with Hook3 suggests that Hook3 might also be associated with pericentriolar satellites. To test this possibility, we examined the ultrastructural localization of Hook3 by immunogold electron microscopy. We used PCM1 antibody in parallel with Hook3 antibody, and found that both antibodies target gold particles to electron-dense granules (approximately 100nm in diameter), whose size and morphology resemble pericentriolar satellites (Figure 4G, arrows). Taken together, these data suggest that Hook3 interacts with PCM1 and both proteins are components of pericentriolar satellites.

Hook3 interacts with PCM1 via its C-terminus

To identify the interaction domain of Hook3 with PCM1, we used different Hook3 fragments (Table in Figure 4A) to perform yeast-two-hybrid interaction assays. We found that the C-terminus of Hook3 (Hook3-C) mediated the binding of the two proteins. To confirm this interaction, we over-expressed flag-tagged Hook3 fragments and GFP-PCM1 in N2A cells, and found that only Hook3-C co-immunoprecipitated with PCM1 (Figure 5A). Furthermore, the amount of PCM1 that co-immunoprecipitated with Hook3 decreased as the expression of Hook3-C increased (Figure 5B). These results indicate that Hook3-C inhibits the interaction between PCM1 and Hook3 in a dominant negative manner.

The Hook3-PCM1 interaction is necessary for proper functioning of pericentriolar satellites

As PCM1 may function as a scaffold for pericentriolar satellites (Dammermann and Merdes, 2002; Hames et al., 2005; Kubo and Tsukita, 2003), we investigated the significance of the Hook3-PCM1 interaction on trafficking of pericentriolar satellites. To this end, we transfected N2A cells with control RNAi, Hook3 RNAi, or Hook3-C, and stained cells with PCM1 antibody. PCM1 is used here as a marker for pericentriolar satellites. In Hook3 RNAi and Hook3-C expressing cells, PCM1-containing granules were dispersed from the centrosomal periphery (Figure 5D, E). We confirmed that total PCM1 levels were unchanged in Hook3 RNAi and Hook3-C expressing cells to exclude the possibility that the loss of centrosomal localization of PCM1 might be due to PCM1 degradation (Figure 5G). Furthermore, PCM1 RNAi dispersed Hook3-containing granules from the centrosomal periphery (Figure 5F). The characterization of PCM1 RNAi is shown in supplemental Figure 3A-C. These results suggest that the Hook3-PCM1 interaction is required for trafficking of pericentriolar satellites towards the centrosome.

Further evidence was obtained by electron microscopy. Transfected cells were sorted by flow cytometry prior to fixation and processed for ultra-thin sectioning. We then collected all sections containing the centrosome and quantified the number of pericentriolar satellites within a square of $16\mu m^2$ surrounding the centrosome (with the centrosome in the center; arrows in Figure 5H;). The high magnification of pericentriolar satellites around the centrosome is shown in Figure 5I. Significantly less pericentriolar satellites were found surrounding the centrosome in Hook3 knockdown cells. A similar phenotype was observed with PCM1 RNAi and Hook3-C over-expression (Figure 5H, J). In summary, these data suggest that disrupting the Hook3-PCM1 interaction impairs the proper functioning of pericentriolar satellites, either by disrupting their assembly or blocking their transport to the centrosome.

The Hook3-PCM1 interaction regulates centrosomal protein assembly and microtubule anchorage to the centrosome

As mentioned above, pericentriolar satellites mediate the assembly of centrosomal proteins (Dammermann and Merdes, 2002). Hence, we tested whether disrupting the Hook3-PCM1 interaction would affect centrosomal protein assembly. We chose to examine the assembly of pericentrin, CDK5Rap2, and ninein, proteins with well-characterized centrosomal functions (Bouckson-Castaing et al., 1996; Doxsey, 2001a). Compared to the control, N2A cells transfected with Hook3 RNAi, PCM1 RNAi, or Hook3-C displayed reduced centrosomal localization of these three proteins (Figure 6A, B).

To further establish the dynamic assembly of these centrosomal proteins, we performed FRAP analysis using CDK5Rap2 as a representative centrosomal protein (Hames et al., 2005; Thompson et al., 2004). In the control, centrosomal venus-CDK5Rap2 recovered to 73% of its original level within 3 minutes. In contrast, Hook3 and PCM1 knockdown significantly reduced the extent of recovery (Figure 6C, D). The minor recovery observed after Hook3 or PCM1 knockdown is likely due to diffusion of proteins from the neighboring cytoplasmic area. These results strongly indicate that Hook3 and PCM1 are essential for the dynamic assembly of centrosomal proteins.

Disruption of the dynamic assembly of pericentriolar material may result in abnormalities in various centrosomal functions. Here, we examined the most well-established functions of the centrosome: microtubule nucleation and anchorage. We chose NIH3T3 given their higher tolerance to nocodazole treatment compared to N2A cells. After transfection with Hook3 RNAi, PCM1 RNAi, or Hook3-C, NIH3T3 cells were treated with nocodazole and allowed to recover after drug washout. Nocodazole depolymerized microtubules and disrupted the trafficking of pericentriolar satellites, resulting in a dispersion of Hook3 and PCM1 from the centrosome (Figure S4A, B). After a 5 min recovery period, most transfected cells (white stars) in both the control and RNAi treated group showed a clear microtubule aster, indicating that initial microtubule nucleation was not affected (Figure 6E, G, Figure S4C). However, after 20 min of recovery, control cells contained clear microtubule asters organized radially from the centrosome (arrowheads), whereas microtubule asters in most Hook3 and PCM1 RNAi and Hook3-C transfected cells were lost (Figure 6F,G, Figure S4D). Taken together, these data suggest that after compromising the function of pericentriolar satellites, microtubule anchorage at the centrosome is impaired, likely due to insufficient targeting of microtubule anchorage proteins to pericentriolar material.

The Hook3-PCM1 interaction regulates embryonic neurogenesis by controlling INM

We next investigated the physiological role of the Hook3-PCM1 interaction in cortical development. We employed two RNAi constructs to silence endogenous PCM1 expression (Figure S3A-C). These RNAi constructs and the dominant negative Hook3-C construct were then introduced into E11.5 embryonic brains by in utero electroporation, and brains were

examined at E14.5. PH3 immunostaining revealed a significantly higher percentage of ectopic mitoses compared to the control (Figure 7A-B). In addition, the ratio of length to width of transfected nuclei was significantly lower (Figure S5A, B). These results suggest that similar to Hook3 knockdown, PCM1 knockdown or disrupting the Hook3-PCM1 interaction impairs INM.

To directly assess involvement of the Hook3-PCM1 interaction in INM, we performed time-lapse imaging of E13.5 acute brain slices. We found that the long distance movement of cell bodies was significantly reduced by PCM1 knockdown or Hook3-C over-expression (Figure S5C, D; movie S5, S6). Taken together, these data suggest that the Hook3-PCM1 interaction is required for neural progenitors to carry out INM.

The interaction between Hook3 and PCM1 is necessary for maintenance of the neural progenitor pool

We next examined involvement of the Hook3-PCM1 interaction in embryonic neurogenesis. The cell cycle exit index was significantly higher and BrdU incorporation lower in brains electroporated with PCM1 RNAi or Hook3-C compared to the control (Figure 7C, D, E). Furthermore, the percentage of cells remaining in the SVZ and VZ was significantly lower; correspondingly, the percentage of cells that migrated to the IZ and CP was significantly higher (Figure S5E, F). In addition, the percentage of Tuj1-posivite or NeuN-positive cells increased, indicating a higher percentage of neurons in the cortex compared to the control (Figure S3, S5G). Taken together these data suggest that following disruption of the PCM1-Hook3 interaction, INM is impaired, leading to a temporary overproduction of neurons and premature depletion of the neural progenitor pool.

Loss of function of Hook3 or PCM1 does not affect intermediate neural progenitors and neural progenitor polarity

Neural progenitors in the VZ give rise to intermediate neural progenitors (INPs) that leave the VZ and undergo terminal divisions in the SVZ or IZ, producing two neurons (Noctor et al., 2004). One possibility consistent with our data is that over-proliferation of INPs due to Hook3 or PCM1 knockdown results in the temporary over-production of neurons. We tested this possibility by staining brain sections with Tbr2, a marker for INPs. Compared to the control, the percentage of Tbr2-positive cells was not significantly different after Hook3 or PCM1 knockdown, or after disrupting the interaction between these two proteins (Figure S6). Hence, the overproduction of neurons is not due to the over-proliferation of INPs.

Neural progenitors in the VZ are highly polarized. They anchor to each other at the apical end-feet on the ventricular surface through adherens junctions, which is important for maintenance of the neurogenic niche. We carefully examined the polarity and adhesion of neural progenitors by immunostaining brain sections with the adherens junction marker N-cadherin and F-actin (Figure S7). We did not find any obvious abnormalities after Hook3 or PCM1 knockdown, or after disrupting the interaction between the two proteins.

DISCUSSION

Various centrosomal proteins have been established to be important factors in normal embryonic brain development. Mutations in genes encoding these proteins cause severe developmental disorders that lead to CNS diseases, such as lissencephaly (Olson and Walsh, 2002), microcephaly (Badano et al., 2005), and schizophrenia (Mackie et al., 2007). Most of these proteins localize to the pericentriolar material, which underscores the importance of the pericentriolar material assembly in normal centrosome function. In this study, we examined the significance of pericentriolar material assembly in embryonic brain development and found

that Hook3 and PCM1 are required for trafficking of pericentriolar satellites. Blocking the Hook3-PCM1 interaction abolished the dynamic assembly of centrosomal proteins, resulting in compromised centrosomal functions. This in turn impaired INM, leading to an overproduction of neurons at the expense of the neural progenitor pool. Our studies underscore the essential function of pericentiolar satellites in embryonic neurogenesis, and provide novel insight into the etiology of centrosome-related neurodevelopmental diseases.

Hook3- and PCM1-mediated dynamic assembly of pericentriolar material is essential for INM

Pericentriolar satellite-mediated protein transport is essential for the dynamic assembly of centrosomal proteins (Dammermann and Merdes, 2002; Hames et al., 2005; Kubo et al., 1999). In this study, we showed that Hook3 localizes to pericentriolar satellites through an interaction with PCM1 (Figure 4). Abolishing the Hook3-PCM1 interaction compromised the dynamic assembly of centrosomal components (Figure 5), which led to detachment of microtubules from the centrosome (Figure 6) and subsequent INM impairment. Based on these data, we propose a model for the dynamic assembly of pericentriolar material during neurogenesis (Figure 7F). In this model, PCM1 functions as a scaffold that recruits multiple centrosome proteins, including Hook3, to pericentriolar satellites. Pericentriolar satellites are then transported to the centrosome along microtubules in a dynein-dependent manner. When the Hook3-PCM1 interaction is disrupted, either the assembly or transport of pericentriolar satellites is impaired, leading to decreased protein assembly into the centrosome. Consequently, microtubules detach from the centrosome due to the lack of microtubule anchorage proteins, resulting in the disruption of nuclear movement during INM. In support of this model, we found that abolishing the Hook3-PCM1 interaction impaired INM (Figure 7, S4).

Our immunostaining and EM data showed decreased localization of pericentriolar satellites around the centrosome after Hook3 knockdown (Fig 5D, 5H). This phenomenon may be attributed to defects in the assembly of pericentriolar satellites at the cell periphery or in their subsequent transport towards the centrosome. Although in the current study we can not unambiguously define whether Hook3 interacts directly with PCM1, we attempted to elucidate the interaction of Hook3 and PCM1 by epistatic analysis. We overexpressed one protein in the context of silencing the other, and examined the distribution of pericentriolar satellites in N2a cells, as well as INM and neuronal production in developing cortices. We did not find any significant difference between single gene knockdown and overexpressing one protein in the context of silencing the other (Data not shown). These data suggest that overexpressing either Hook3 or PCM1 in the context of silencing the other gene does not rescue the defects in the trafficking of pericentriolar satellites. We speculate that while PCM1 functions as a scaffold for pericentriolar satellites, Hook3 may mainly function in the transport step, but its recruitment to the pericentriolar satellite relies on PCM1.

Hook3 and PCM1 regulate neurogenesis through INM

Disruption of INM by *in vivo* knockdown of Hook3 or PCM1 resulted in mitoses away from the ventricular surface. After this ectopic division, both daughter cells differentiate into neurons. This results in premature depletion of the neural progenitor pool, which is normally used up at later developmental stages. Similar phenotypes have been reported in other studies when INM is impaired by Lis1 loss-of-function, or by compromising centrosome function through knockdown of centrosomal proteins (Gambello et al., 2003; Xie et al., 2007). A mathematical simulation based on a gradient of Notch signaling in the VZ predicts similar results (Murciano et al., 2002).

Why does ectopic cell division produce two neurons? During apical division, cells are exposed to neural inhibition signals such as Notch, which displays an apical-basal gradient in developing

epithelia (Del Bene et al., 2008; Murciano et al., 2002). Ectopic divisions free cells from this inhibition, resulting in neuronal differentiation. Thus, INM may be a strategy used by the developing cortex to maintain a sufficient neural progenitor pool size during early developmental stages to ensure that the correct number of neurons is generated with temporal precision.

We performed several control experiments to ensure that other properties of neural progenitors were not affected by Hook3 or PCM1 knockdown. First, FACS analysis revealed that Hook3 knockdown did not affect cell cycle progression (Figure S2). Second, the polarity of neural progenitors is not affected, as evidenced by the intact adhesion and polarity of progenitors (Figure S6). We also found that apical processes attaching neural progenitors to the ventricular surface were not affected in knockdown cells (Figure 2F, S4A). Finally, we exclude the possibility that overproduction of neurons may be caused by over-proliferation of Tbr2-positive INPs (Figure S5). These results are consistent with our finding that the neural progenitor pool was depleted.

Functions of the centrosomal proteins in brain development and diseases

Multiple centrosomal proteins have been implicated in human brain development diseases, such as Lis1 (Lissencephaly), ASPM and CDK5Rap2 (microcephaly), Cep290 (Joubert Syndrome). A fraction of DISC1, the protein strongly associated with schizophrenia, also localize to the centrosome (Kamiya et al., 2005; Morris et al., 2003). Both Cep290 and DISC1 interact with two components of the pericentriolar satellite, BBS4 and PCM1 (Kamiya et al., 2005; Kim et al., 2008), suggesting that these two proteins might be the cargo of pericentriolar satellites. In addition, our study established the dependence of the centrosomal assembly of CDK5Rap2 on pericentriolar satellites. Furthermore, recent human genetic studies revealed that the PCM1 gene locus on chromosome 8p22 is strongly associated with schizophrenia (Datta et al., 2008; Gurling et al., 2006; Kamiya et al., 2008). Both DISC1- and PCM1-associated schizophrenic patients show reduced gray matter volume as revealed by magnetic resonance imaging (MRI) studies (Gurling et al., 2006; van Haren et al., 2004), suggesting a possible contribution of impaired neurogenesis to the onset of schizophrenia. In line with this, our previous study showed that DISC1 loss of function results in premature depletion of the neural progenitor pool in early embryonic developmental stages (Mao et al., 2009). In the current study, we showed that compromising PCM1 function leads to similar neurogenesis defects. Taken together, these findings suggest that pericentriolar satellite-mediated centrosomal protein assembly is a general mechanism for the proper functioning of the centrosome in embryonic brain development. Compromising this protein assembly may result in disturbance of multiple events during embryonic brain development, which eventually leads to CNS diseases. For the first time, our study revealed the significance of centrosome protein assembly in embryonic brain development, providing novel insight into the understanding of brain development and diseases.

Experimental Procedures

Plasmids

RNAi plasmids were generated by inserting complementary hairpin oligonucleotides into pSilencer 2.0-U6 (Ambion). Hook3 RNAi-2, and PCM1 RNAI-1, and -2 were obtained from the Mission shRNA library (Sigma). A random sequence without homology to any known mRNA was used as the control RNAi. The Hook3 rescue construct was cloned using the human full-length Hook3 coding sequence; it is resistant to Hook3 RNAi-1 because the latter targets to the 3′-UTR of mouse Hook3. Human Hook3 constructs were provided by H. Kramer (Univ. Texas Southwestern medical center, Dallas, Texas). The EGFP-PCM1 plasmid was provided by A. Merdes (Institute of Science and Technology, Toulouse, France).

In utero eletroporation

Venus plasmid (final concentration 1μg/μl) was co-injected with RNAi plasmid (final concentration 3μg/μl). For triple-electroporations, a mixture of venus, Hook3 RNAi, and wild-type Hook3 was prepared at a ratio of 1:3:3. After pregnant females (Swiss Webster, TACONIC) were anesthetized, embryos were exposed within the uterus, approximately 1μl DNA solution was injected into the lateral ventricle, and electroporation was performed (35 V for 50 ms, with 950ms intervals; 5 pulses). Embryos were then placed back into the abdominal cavity and the abdominal wall was sutured. For BrdU labeling experiments, in utero electroporation was performed at E11.5 and BrdU was injected once at 50 mg/g body weight intraperitoneally at E13.5. Embryos were harvested 3 days after electroporation. Brains were removed and fixed in 4% paraformaldehyde overnight, followed by cryoprotection in 30% sucrose in PBS overnight. Afterwards, brains were embedded in OCT and frozen in liquid nitrogen, and sliced into 12-20μm coronal sections.

Acute brain slice preparation and imaging

Mouse embryos were electroporated at E11.5 and sacrificed at E14.5. Embryonic brains were excised and embedded in 3% low melt agarose (SIGMA, Type VII) and sectioned (coronal, 200μm) using a Vibrotome (Leica VT1000S). Slices were laid on a Millicell culture insert (Millipore) and cultured in Neurobasal medium (supplemented with 1% penicillin-streptomycin, 1% glutamine, N2, B27, and 5% horse serum) at 37°C for 1 hr. Thereafter, brain sections were viewed through a 20X objective (NA 0.75) of a Nikon inverted microscope linked to a DeltaVision deconvolution-imaging system (Applied Precision). Images were collected every 10 min for 6-8 hr.

Immunohistochemistry and immunocytochemistry

For cryosections, brain slices were incubated in blocking solution (2% goat serum, 0.2% Triton X-100 in PBS) for 1 hr at room temperature. For BrdU staining, brain sections were incubated in 4N HCl solution for 2 hr at room temperature to unmask the antigen, followed by three washes in PBS. Subsequently, brain sections were blocked and incubated in primary antibodies diluted in blocking solution for 2 hr at room temperature, or 24 hr at 4°C. Primary antibodies used were anti-Hook3 (kindly provided by H. Kramer), anti-nestin (Rat401, 1:500; BD Pharmingen), anti-Tuj1 (monoclonal, 1:1000, Covance), anti-pericentrin (monoclonal, 1:100, BD Biosciences), anti-phospho histone H3 (polyclonal, 1:500, Upstate), anti-BrdU (monoclonal, 1:500, Dakocytomation), anti-Ki67 (poluclonal, 1:500, Neomarkers), anti-α-tubulin (1:1000, Sigma T5168), anti-PCM1 (polyclonal, 1:500, kindly provided by A. Merdes), anti-GFP (Chicken polyclonal, 1:1000, Aves Labs). Sections were then washed three times with PBS and incubated with secondary antibody against goat IgG conjugated to cy2, or cy3, or cy5 (1:500, Jackson ImmunoResearch), followed by staining with Hoechst 33258 (Sigma). Sections were mounted with Antifade reagent (Invitrogen) for fluorescence microscopy.

Electron microscopy

N2A cells were cotransfected with Venus and the indicated plasmids, and sorted by FACS to enrich for GFP positive cells the following day. Cells were fixed after a 2 day recovery period. For conventional EM, cells were fixed in 2.5% paraformaldehyde and 2.5% glutaraldehyde in PBS PH 7.4 for 10 min at room temperature, followed by three washes in PBS. Samples were then postfixed with 1% osmiumtetroxide/1.5% potassium ferrocyanide (in H_2O) for 1 hour at room temperature in the dark, followed by three washes in water. Next, samples were incubated in 1% uranyl acetate (in H2O) for 30 min, and then dehydrated through an ethanol series, infiltrated in a 1:1 solution of propylene oxide and epon, and finally embedded in pure epon overnight at 60°C. Sections were prepared using an ultramicrotome (Reichert Ultracut –S),

collected on Formvar-coated copper grids, post-stained at room temperature with 2% aqueous uranyl acetate, and treated with 0.2% lead citrate for 15 min.

For immuno-gold staining, cells were fixed in 4% paraformaldehyde in PBS for 10 min at room temperature, and permeabilized in 0.2% Triton X-100 in PBS for 10 min at room temperature. Samples were then blocked in 1% BSA in PBS for 30 min, and incubated in primary antibody (Rabbit anti-Hook3, 1:50; Rabbit anti-PCM1, 1:50) at 4°C overnight. After three washes in PBS, samples were incubated in 5nm colloidal gold-conjugated Protein A for 1-2 hr at room temperature. After 5 washes in PBS, samples were post-fixed in 2.5% glutaraldehyde in 0.1M cacodylate buffer pH7.4 for 0.5-1 hr. Samples were then processed as described above. Sections were observed and photographed on an electron microscope (Tecnai™ G^2 Spirit BioTWIN).

Fluorescence recovery after photobleaching (FRAP)

NIH3T3 cells were transfected with venus-CDK5rap2 together with corresponding RNAis, and plated on glass-bottom dishes. FRAP was performed 3 days later with a Zeiss LSM 510 confocal microscope using a 63X water lens. A small region of interest of about 2μm in diameter centered on the centrosome was bleached with 10 iterations and 100% laser power (488-nm argon laser). Two images were captured before bleaching. After bleaching, images were taken every 2 seconds (488-nm argon laser at 2% power) over a 200 second period. At each time point, the fluorescence intensity of the photobleached area (P1) and an unbleached area of the same size in the cytoplasm were measured with LSM 510 software. Fluorescence intensity was normalized as B1/B2. Background fluorescence was defined as the normalized intensity of the first frame after photobleaching, and this value was subtracted from all frames to obtain the final fluorescence intensity of the ROI (Proi =B1/B2 - BI). Fluorescence recovery of a given time point was calculated as the final fluorescence intensity (Proi) divided by the final fluorescence intensity of the frame immediately prior to photobleaching.

Supplementary Material

Refer to Web version on PubMed Central for supplementary material.

Acknowledgments

REFERENCES

Badano JL, Teslovich TM, Katsanis N. The centrosome in human genetic disease. Nat Rev Genet 2005;6:194–205. [PubMed: 15738963]

Balczon R, Bao L, Zimmer WE. PCM-1, A 228-kD centrosome autoantigen with a distinct cell cycle distribution. J Cell Biol 1994;124:783–793. [PubMed: 8120099]

Baron AT, Salisbury JL. Identification and localization of a novel, cytoskeletal, centrosome-associated protein in PtK2 cells. J Cell Biol 1988;107:2669–2678. [PubMed: 3060471]

Baron AT, Suman VJ, Nemeth E, Salisbury JL. The pericentriolar lattice of PtK2 cells exhibits temperature and calcium-modulated behavior. J Cell Sci 1994;107(Pt 11):2993–3003. [PubMed: 7698999]

Berns MW, Rattner JB, Brenner S, Meredith S. The role of the centriolar region in animal cell mitosis. A laser microbeam study. J Cell Biol 1977;72:351–367. [PubMed: 556728]

Bettencourt-Dias M, Glover DM. Centrosome biogenesis and function: centrosomics brings new understanding. Nat Rev Mol Cell Biol 2007;8:451–463. [PubMed: 17505520]

Bouckson-Castaing V, Moudjou M, Ferguson DJ, Mucklow S, Belkaid Y, Milon G, Crocker PR. Molecular characterisation of ninein, a new coiled-coil protein of the centrosome. J Cell Sci 1996;109 (Pt 1):179–190. [PubMed: 8834802]

Chenn A, McConnell SK. Cleavage orientation and the asymmetric inheritance of Notch1 immunoreactivity in mammalian neurogenesis. Cell 1995;82:631–641. [PubMed: 7664342]

Cohen E, Binet S, Meininger V. Ciliogenesis and centriole formation in the mouse embryonic nervous system. An ultrastructural analysis. Biol Cell 1988;62:165–169. [PubMed: 3390625]

Dammermann A, Merdes A. Assembly of centrosomal proteins and microtubule organization depends on PCM-1. J Cell Biol 2002;159:255–266. [PubMed: 12403812]

Datta SR, McQuillin A, Rizig M, Blaveri E, Thirumalai S, Kalsi G, Lawrence J, Bass NJ, Puri V, Choudhury K, et al. A threonine to isoleucine missense mutation in the pericentriolar material 1 gene is strongly associated with schizophrenia. Mol Psychiatry. 2008

Del Bene F, Wehman AM, Link BA, Baier H. Regulation of neurogenesis by interkinetic nuclear migration through an apical-basal notch gradient. Cell 2008;134:1055–1065. [PubMed: 18805097]

Doxsey S. Re-evaluating centrosome function. Nat Rev Mol Cell Biol 2001a;2:688–698. [PubMed: 11533726]

Doxsey SJ. Centrosomes as command centres for cellular control. Nat Cell Biol 2001b;3:E105–108. [PubMed: 11331889]

Gambello MJ, Darling DL, Yingling J, Tanaka T, Gleeson JG, Wynshaw-Boris A. Multiple dose-dependent effects of Lis1 on cerebral cortical development. J Neurosci 2003;23:1719–1729. [PubMed: 12629176]

Gurling HM, Critchley H, Datta SR, McQuillin A, Blaveri E, Thirumalai S, Pimm J, Krasucki R, Kalsi G, Quested D, et al. Genetic association and brain morphology studies and the chromosome 8p22 pericentriolar material 1 (PCM1) gene in susceptibility to schizophrenia. Arch Gen Psychiatry 2006;63:844–854. [PubMed: 16894060]

Hames RS, Crookes RE, Straatman KR, Merdes A, Hayes MJ, Faragher AJ, Fry AM. Dynamic recruitment of Nek2 kinase to the centrosome involves microtubules, PCM-1, and localized proteasomal degradation. Mol Biol Cell 2005;16:1711–1724. [PubMed: 15659651]

Higginbotham HR, Gleeson JG. The centrosome in neuronal development. Trends Neurosci 2007;30:276–283. [PubMed: 17420058]

Kamiya A, Kubo K, Tomoda T, Takaki M, Youn R, Ozeki Y, Sawamura N, Park U, Kudo C, Okawa M, et al. A schizophrenia-associated mutation of DISC1 perturbs cerebral cortex development. Nat Cell Biol 2005;7:1167–1178. [PubMed: 16299498]

Kamiya A, Tan PL, Kubo K, Engelhard C, Ishizuka K, Kubo A, Tsukita S, Pulver AE, Nakajima K, Cascella NG, et al. Recruitment of PCM1 to the centrosome by the cooperative action of DISC1 and BBS4: a candidate for psychiatric illnesses. Arch Gen Psychiatry 2008;65:996–1006. [PubMed: 18762586]

Khodjakov A, Rieder CL. The sudden recruitment of gamma-tubulin to the centrosome at the onset of mitosis and its dynamic exchange throughout the cell cycle, do not require microtubules. J Cell Biol 1999;146:585–596. [PubMed: 10444067]

Kim J, Krishnaswami SR, Gleeson JG. CEP290 interacts with the centriolar satellite component PCM-1 and is required for Rab8 localization to the primary cilium. Hum Mol Genet 2008;17:3796–3805. [PubMed: 18772192]

Kim JC, Badano JL, Sibold S, Esmail MA, Hill J, Hoskins BE, Leitch CC, Venner K, Ansley SJ, Ross AJ, et al. The Bardet-Biedl protein BBS4 targets cargo to the pericentriolar region and is required for microtubule anchoring and cell cycle progression. Nat Genet 2004;36:462–470. [PubMed: 15107855]

Kubo A, Sasaki H, Yuba-Kubo A, Tsukita S, Shiina N. Centriolar satellites: molecular characterization, ATP-dependent movement toward centrioles and possible involvement in ciliogenesis. J Cell Biol 1999;147:969–980. [PubMed: 10579718]

Kubo A, Tsukita S. Non-membranous granular organelle consisting of PCM-1: subcellular distribution and cell-cycle-dependent assembly/disassembly. J Cell Sci 2003;116:919–928. [PubMed: 12571289]

Luders J, Stearns T. Microtubule-organizing centres: a re-evaluation. Nat Rev Mol Cell Biol 2007;8:161–167. [PubMed: 17245416]

Mackie S, Millar JK, Porteous DJ. Role of DISC1 in neural development and schizophrenia. Curr Opin Neurobiol 2007;17:95–102. [PubMed: 17258902]

Malone CJ, Misner L, Le Bot N, Tsai MC, Campbell JM, Ahringer J, White JG. The C. elegans hook protein, ZYG-12, mediates the essential attachment between the centrosome and nucleus. Cell 2003;115:825–836. [PubMed: 14697201]

Mao Y, Ge X, Frank CL, Madison JM, Koehler AN, Doud MK, Tassa C, Berry EM, Soda T, Singh KK, et al. Disrupted in schizophrenia 1 regulates neuronal progenitor proliferation via modulation of GSK3beta/beta-catenin signaling. Cell 2009;136:1017–1031. [PubMed: 19303846]

Messier PE, Auclair C. Effect of cytochalasin B on interkinetic nuclear migration in the chick embryo. Dev Biol 1974;36:218–223. [PubMed: 4822837]

Miyama S, Takahashi T, Goto T, Bhide PG, Caviness VS Jr. Continuity with ganglionic eminence modulates interkinetic nuclear migration in the neocortical pseudostratified ventricular epithelium. Exp Neurol 2001;169:486–495. [PubMed: 11358462]

Morris JA, Kandpal G, Ma L, Austin CP. DISC1 (Disrupted-In-Schizophrenia 1) is a centrosome-associated protein that interacts with MAP1A, MIPT3, ATF4/5 and NUDEL: regulation and loss of interaction with mutation. Hum Mol Genet 2003;12:1591–1608. [PubMed: 12812986]

Murciano A, Zamora J, Lopez-Sanchez J, Frade JM. Interkinetic nuclear movement may provide spatial clues to the regulation of neurogenesis. Mol Cell Neurosci 2002;21:285–300. [PubMed: 12401448]

Noctor SC, Martinez-Cerdeno V, Ivic L, Kriegstein AR. Cortical neurons arise in symmetric and asymmetric division zones and migrate through specific phases. Nat Neurosci 2004;7:136–144. [PubMed: 14703572]

Olson EC, Walsh CA. Smooth, rough and upside-down neocortical development. Curr Opin Genet Dev 2002;12:320–327. [PubMed: 12076676]

Paoletti A, Moudjou M, Paintrand M, Salisbury JL, Bornens M. Most of centrin in animal cells is not centrosome-associated and centrosomal centrin is confined to the distal lumen of centrioles. J Cell Sci 1996;109(Pt 13):3089–3102. [PubMed: 9004043]

Rieder CL, Faruki S, Khodjakov A. The centrosome in vertebrates: more than a microtubule-organizing center. Trends Cell Biol 2001;11:413–419. [PubMed: 11567874]

Ross CA, Margolis RL, Reading SA, Pletnikov M, Coyle JT. Neurobiology of schizophrenia. Neuron 2006;52:139–153. [PubMed: 17015232]

Sauer F. Mitosis in the Neural Tube. Journal of Comparative Neurology 1935;62:337–420.

Thompson HM, Cao H, Chen J, Euteneuer U, McNiven MA. Dynamin 2 binds gamma-tubulin and participates in centrosome cohesion. Nat Cell Biol 2004;6:335–342. [PubMed: 15048127]

Tsai JW, Chen Y, Kriegstein AR, Vallee RB. LIS1 RNA interference blocks neural stem cell division, morphogenesis, and motility at multiple stages. J Cell Biol 2005;170:935–945. [PubMed: 16144905]

Valente EM, Silhavy JL, Brancati F, Barrano G, Krishnaswami SR, Castori M, Lancaster MA, Boltshauser E, Boccone L, Al-Gazali L, et al. Mutations in CEP290, which encodes a centrosomal protein, cause pleiotropic forms of Joubert syndrome. Nat Genet 2006;38:623–625. [PubMed: 16682970]

van Haren NE, Picchioni MM, McDonald C, Marshall N, Davis N, Ribchester T, Pol H.E. Hulshoff, Sharma T, Sham P, Kahn RS, Murray R. A controlled study of brain structure in monozygotic twins concordant and discordant for schizophrenia. Biol Psychiatry 2004;56:454–461. [PubMed: 15364044]

Webster W, Langman J. The effect of cytochalasin B on the neuroepithelial cells of the mouse embryo. Am J Anat 1978;152:209–221. [PubMed: 567005]

Xie Z, Moy LY, Sanada K, Zhou Y, Buchman JJ, Tsai LH. Cep120 and TACCs control interkinetic nuclear migration and the neural progenitor pool. Neuron 2007;56:79–93. [PubMed: 17920017]

Young A, Dictenberg JB, Purohit A, Tuft R, Doxsey SJ. Cytoplasmic dynein-mediated assembly of pericentrin and gamma tubulin onto centrosomes. Mol Biol Cell 2000;11:2047–2056. [PubMed: 10848628]

Zimmerman W, Doxsey SJ. Construction of centrosomes and spindle poles by molecular motor-driven assembly of protein particles. Traffic 2000;1:927–934. [PubMed: 11208082]
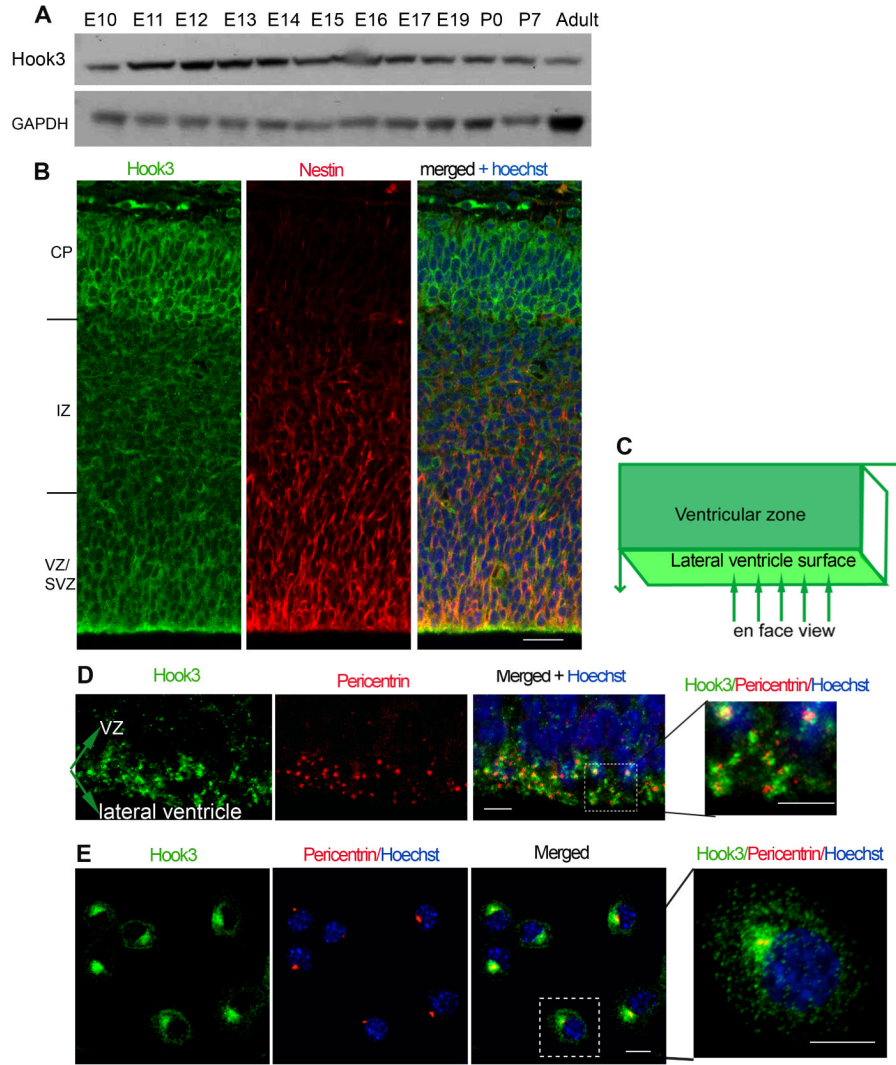
Figure 1. Mouse Hook3 localizes to the periphery of the centrosome
(A) Western blot of brain lysates from various developmental stages. (B) Immunostaining of E14 brain sections. Hook3 (green) is highly expression in CP and VZ. In the VZ, Hook3 is expressed by nestin-positive neural progenitors. (C) Diagram of en face view of the ventricular surface. (D) En face view of Hook3 expression pattern at the ventricular surface. (E) N2A cells immunostained for Hook3 and pericentrin. The enlarged cell shows that Hook3 localizes to granular structures that concentrate to the centrosome. Scale bars: 50 μm in B; 10 μm in D-E. See also Figure S1.
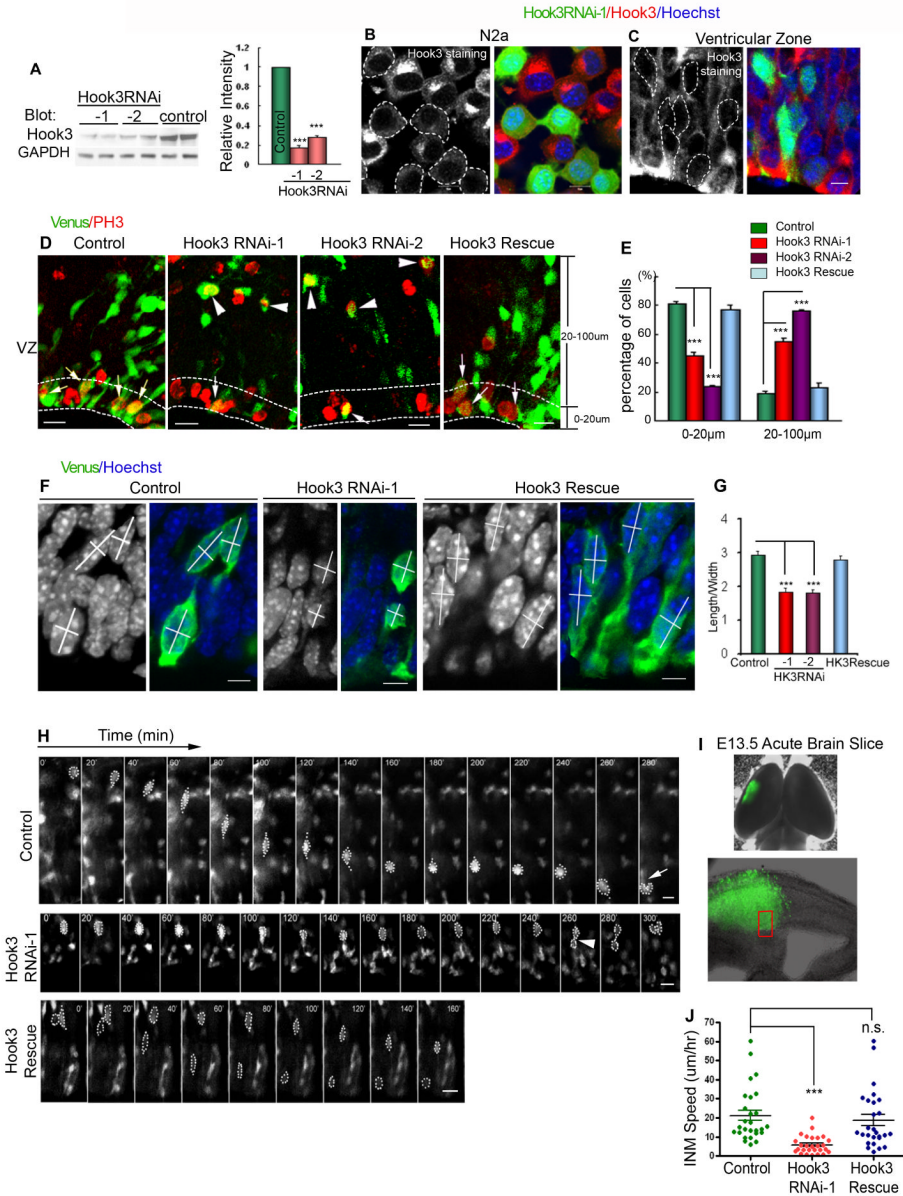
Figure 2. Hook3 regulates interkinetic nuclear migration (INM)

(A) Hook3 RNAi silenced endogenous protein expression in N2A cells three days after transfection. Densitometry was performed with ImageJ software (n=4). (B-C) Immunostaining of N2A cells and brain slices 3 days after Hook3 RNAi transfection. Hook3 protein levels are lower in cells transfected with Hook3 RNAi (dashed circles). In Figure D-F, in utero electroporations were performed at E11.5 and brains were examined at E14.5. (D-E) Hook3 knockdown leads to mitosis away from the ventricular surface. Mitosis within 20 μm (indicated by dashed lines) from the ventricular surface is considered apical division, and mitosis in the 20-100 μm zone is considered ectopic cell division (n=3-4). (F) Nuclei assume round shapes after Hook3 knockdown. (G) Quantification showing the ratio of nuclear length to width (indicated by white lines in F) (n=15-18). (H-J) Hook3 knockdown impairs INM in acute brain slices. Mice were electroporated at E11.5 and sacrificed at E13.5. (H) Time-lapse video sequences of cells undergoing INM in control, Hook3 RNAi, and Hook3-rescued cortical

slices. Ventricular surface is located at the bottom of the images. Time is denoted in the upper left corner. Cell bodies are delineated by dashed lines. Arrows indicate mitosis at the apical surface; arrowheads indicate ectopic mitosis. The red box in (I) represents the imaging area (n=27). Data are presented as mean±SEM. **p<0.01, ***p<0.001, one-way ANOVA. Scale bars: 10 μm in B-C, F; 20 μm in D and H.
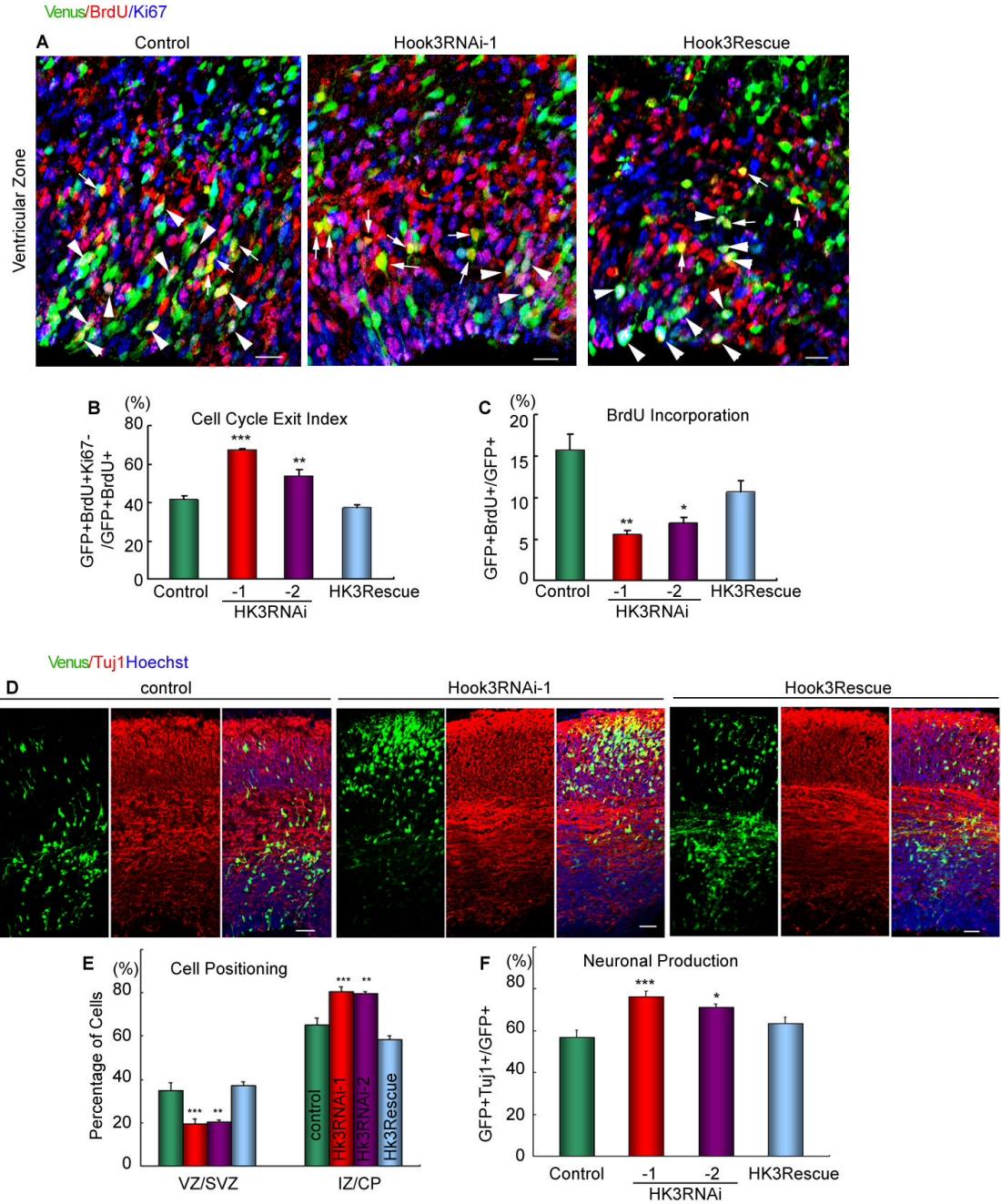
Venus/BrdU/Ki67

A Control   Hook3RNAi-1   Hook3Rescue

Ventricular Zone

B (%) Cell Cycle Exit Index

C (%) BrdU Incorporation

Venus/Tuj1Hoechst

D control   Hook3RNAi-1   Hook3Rescue

CP
IZ
ZV/
SVZ

E (%) Cell Positioning

F (%) Neuronal Production

Figure 3. Hook3 is required for maintenance of the neural progenitor pool
(A) Mice were electroporated at E11.5, pulse labeled with BrdU at E13.5, and sacrificed at
E14.5. Brain sections were then stained with antibodies against BrdU, Ki67 (blue), and GFP
(green). GFP-positive cells labeled with both BrdU and Ki67 (white arrowheads) remain in the
cell cycle; GFP-positive cells labeled with BrdU but not Ki67 (white arrows) have exited the
cell cycle. Total BrdU incorporation in transfected cells (sum of arrows and arrow heads)
decreases after Hook3 knockdown. (B) Quantification of cell cycle exit index (n=5-7). (C)
Quantification of BrdU incorporation index (n=5-7). (D) Mice were electroporated at E11.5
and sacrificed at E14.5. Hook3 knockdown leads to a higher percentage of transfected cells
that have migrated to the CP and IZ, and a lower percentage of cells remaining in the VZ and

SVZ. (E) Quantification of cell positioning (n=3-5). (F) Quantification of Tuj1-positive cells (n=3-5). Data are presented as mean ± SEM. *p < 0.05, **p <0.01, ***p<0.001(one-way ANOVA). Scale bars: 20 μm in A; 50 μm in D.
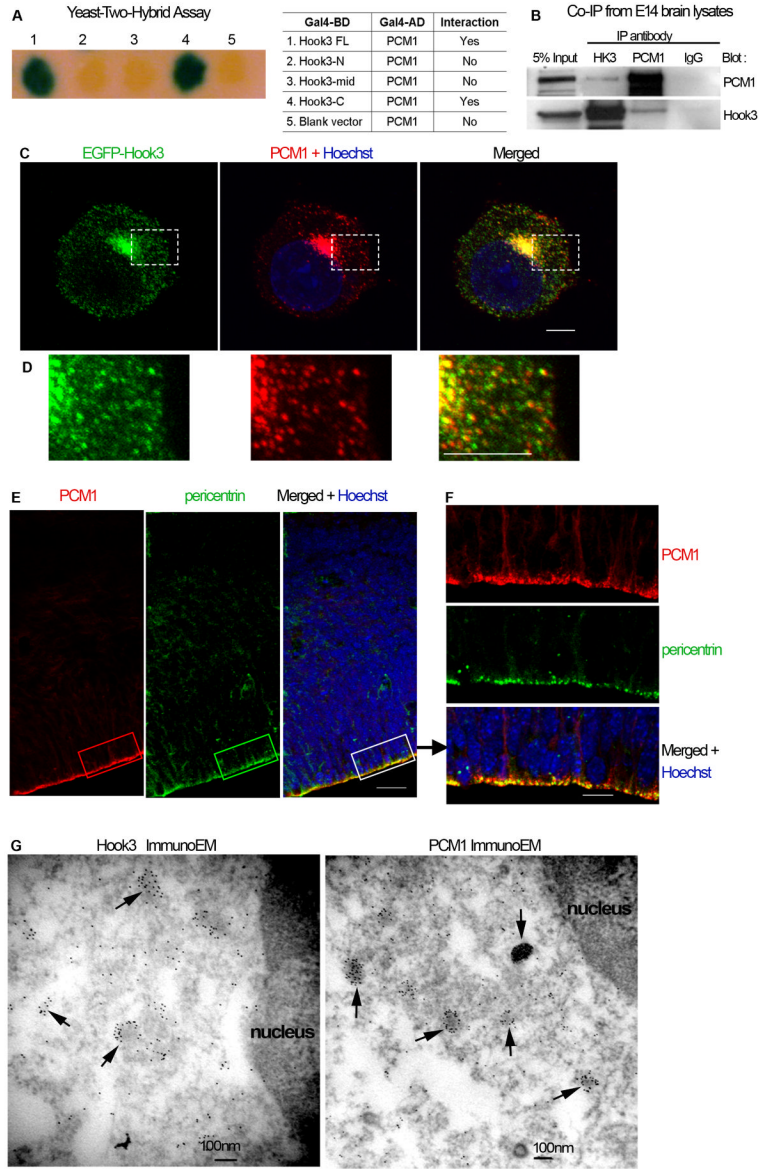
Figure 4. Hook3 interacts with PCM1 and localizes to pericentriolar satellites
(A) β-gal assay using the yeast-two-hybrid system. Fragments of Hook3 were fused with the gal4-binidng domain, and PCM1 was fused with the gal4-activating domain. Blue colonies indicate that the two proteins interact. Hook3-N: N-terminal 170aa; Hook3-C: C-terminal 170aa; Hook3-mid: the remaining middle portion of the protein. (B) Co-IP results using E14 brain lysates. (C) EGFP-Hook3 was overexpressed in N2A cells and the cells were stained with anti-PCM1. (D) Enlarged square area in (C) showing the overlap of EGFP-Hook3 and PCM1 immunofluorescence. (E) Vibratome sections (50 μm) were stained with PCM1 and pericentrin (green) antibodies. PCM1 highlights the apical surface of the VZ. (F) Boxed area in (E) showing the overlap of PCM1 with pericentrin at the ventricular surface. (G) Immunogold EM analysis of N2A cells revealed that Hook3 and PCM1 localize to pericentriolar satellites (black arrows). Gold particles were 5nm. Scale bars: 5 μm in C, D; 50 μm in E; 30 in F; 100 nm in G.
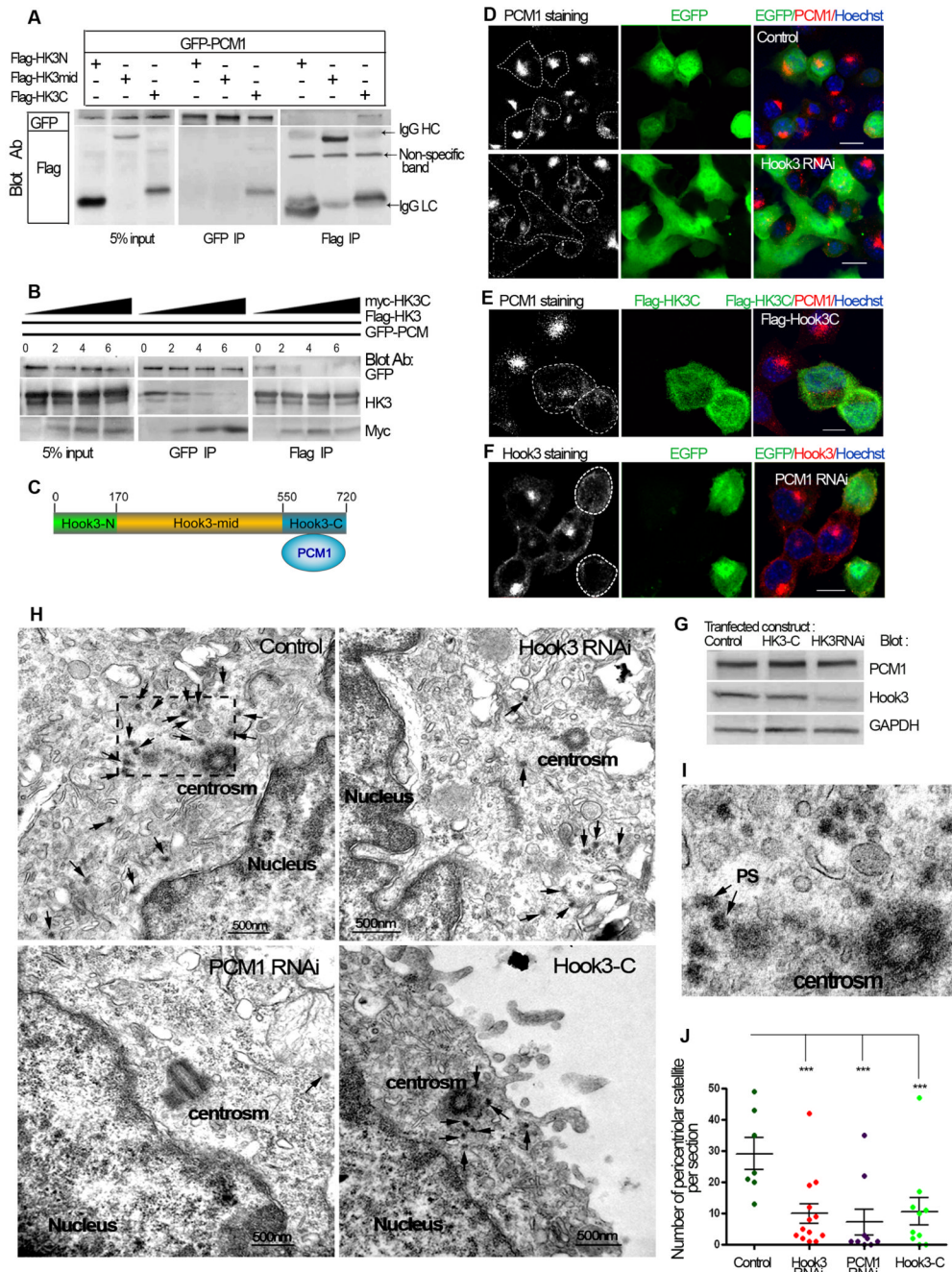
Figure 5. Hook3-PCM1 interaction is necessary for the proper functioning of pericentriolar satellites

(A) GFP-PCM1 and flag-tagged Hook3 fragments were co-expressed in N2A cells. Only Hook3-C co-immunoprecipitates with PCM1. (B) Hook3-C affects the interaction between Hook3 and PCM1 in a dominant negative manner. GFP-PCM1 and flag-Hook3 were transfected at a constant ratio, while myc-Hook3C was transfected at increasing levels (0 to 6-fold of myc-Hook3). (C) Diagram showing that the C-terminus of Hook3 binds to PCM1. (D) N2A cells were transfected with control or Hook3 RNAi together with EGFP and stained with PCM1 antibody. PCM1 disperses from the centrosome after Hook3 knockdown. (E) N2A cells transfected with flag-Hook3C and stained with anti-flag (green) and anti-PCM1 antibodies.

Hook3C shows diffusive distribution throughout the cytoplasm, and it also disperses PCM1 from the centrosome. (F) PCM1 RNAi similarly disperses Hook3 from the centrosome. (G) The same batch of cells in (D-E) were lysed and subjected to western blot. Total PCM1 levels do not change after Hook3 knockdown or Hook3-C overexpression. (H) Conventional EM images. Pericentriolar satellites (black arrows) were identified as electron dense granules surrounding the centrosome. (I) The zoomed-in image of the square area in the control cell, showing representative pericentriolar satellites surrounding the centrosome. (J) Quantification of pericentriolar satellites on 16 μm^2 square size with the centrosome in the center (n=7, 13, 9, 10 for control, Hook3 RNAi, PCM1 RNAi, Hook3-C respectively). Data are presented as mean ± SEM.***p<0.001 (Mann-Whitney test). Scale bars: 10 μm in D-F; 500 nm in H. centrosm: centrosome. PS: pericentriolar satellite.
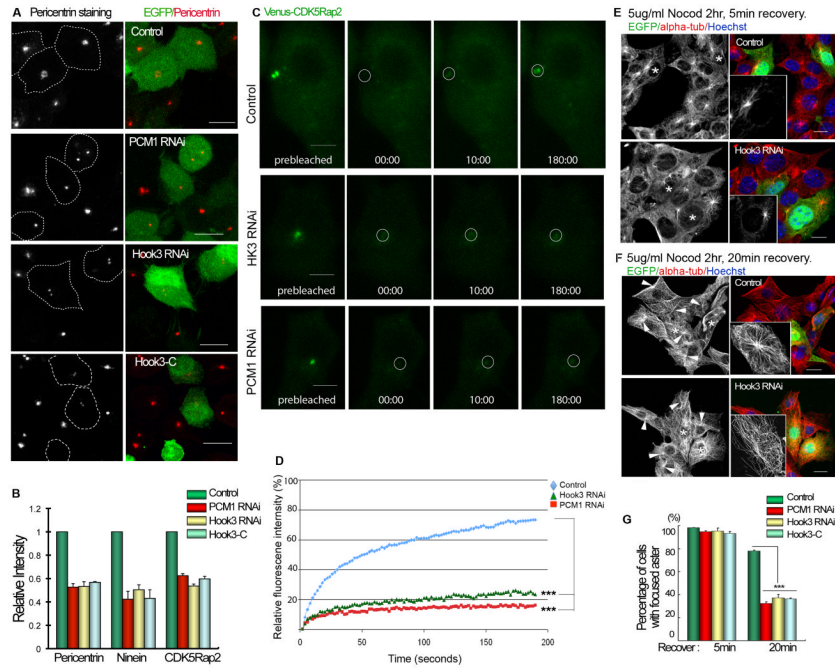
Figure 6. Hook3-PCM1 interaction is required for centrosomal protein assembly and microtubule anchorage to the centrosome

(A) N2A cells were transfected with corresponding constructs (circled by white dashed lines), and immunostained with an antibody against pericentrin. Images are projections of confocal image stacks. (B) Relative intensities of pericentrin, ninein, and CDk5Rap2 at the centrosome. Ratio represents protein intensity in the centrosome over that at the cell periphery. Measurements were performed with ImageJ (n=30-40 cells). (C) Venus-CDK5rap2 was expressed in NIH3T3 cells together with corresponding constructs. FRAP experiments were performed on cells with low expression levels to avoid protein aggregates. Time labels indicate time after photobleaching. (D) Quantification of venus-CDK5rap2 recovery after photobeaching. Each data point represents the average intensity of 8 cells. (E) NIH3T3 cells were transfected with corresponding constructs (transfected cells are marked by white stars). 3 days later, cells were incubated with 5ug/ml nocodazole for 2 hr. After a 5 minute recovery period, most cells have a well-focused microtubule aster, indicating that microtubule nucleation is normal. Insets are zoom-in images of representative cells with newly formed microtubule asters. (F) After a 20 minute recovery period, control cells have a well focused radial microtubule structures (arrow heads, and inset), whereas in Hook3 knockdown cells, microtubules are unfocused (inset). (G) Quantification of cells with focused microtubule asters. (n=3, 150-200 cells are quantified). Data are presented as mean ± SEM.***p<0.001(one-way ANOVA). Scale bars: 10µm. See also Figure S3 and S4.
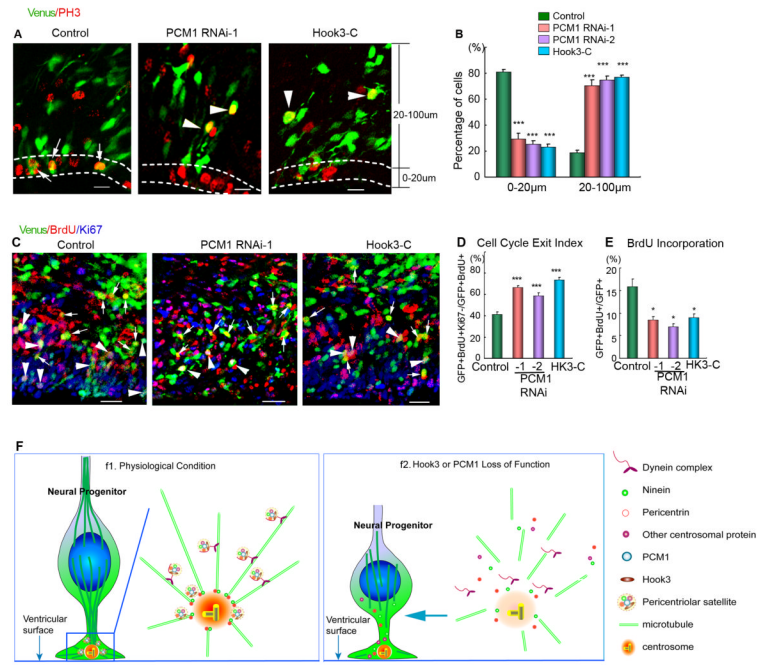
Figure 7. PCM1-Hook3 interaction is required for INM and maintenance of the neural progenitor pool

(A) PCM1 knockdown leads to mitosis away from the ventricular surface. White arrows mark apical divisions; arrowheads marked ectopic division. (B) Quantification of the distribution of PH3-positive cells in different zones (n=3-4). (C) Cell cycle exit assay. See Figure 3A for experimental procedure. (D) Cell cycle exit index (n=4-7). (E) BrdU incorporation index (n=4-7). (F) A model to explain functions of Hook3 and PCM1 in neural progenitors. (f1) In physiological conditions, PCM1 functions as a scaffold and recruits multiple proteins, including Hook3, to form pericentriolar satellites. Pericentriolar satellites are subsequently transported along microtubules in a dynein-dependent manner, and finally deliver the proteins to the centrosome. (f2) Under conditions of Hook3 or PCM1 loss of function, or after the Hook3-PCM1 interaction is disrupted, the assembly or transport of pericentriolar satellites is impaired. This leads to defects in the dynamic assembly of the centrosome. Subsequently, various centrosome functions are compromised, including its ability to organize microtubules. The net result is the disruption of INM, which eventually results in neurogenesis defects. Data are presented as mean ± SEM. *$p<0.05$, **$p<0.01$, ***$p<0.001$, one-way ANOVA. Scale bars: 20 μm in A; 50 μm in C. See also Figure S5.